UHF RFID Localization Based on Evaluation of Backscattered Tag Signals

Martin Scherhäufl, *Graduate Student Member, IEEE*, Markus Pichler, *Member, IEEE*, and Andreas Stelzer, *Member, IEEE*

***Abstract*— This paper introduces a 2-D position measurement system for passive ultra-high frequency (UHF) radio frequency identification (RFID) tags based on evaluation of backscattered transponder signals. The main application of the system is the localization of stationary objects tagged with RFID transponders. By combining phase and amplitude evaluation, the accuracy and the robustness of the position estimates are significantly improved compared with either approach alone. A multiple input multiple output system in which, sequentially, each frontend is configured to work as a transmitter while the remaining frontends serve as receivers is used to enable position estimation. For proof of concept, a local position measurement system demonstrator was built comprising conventional passive EPCglobal Class-1 Gen-2 UHF RFID tags, a commercial off-the-shelf RFID reader, eight transceiver frontends, baseband hardware, and signal processing. Measurements were carried out in an indoor office environment where the 3.5 m × 2.5 m measurement zone was surrounded by drywalls and concrete floor and ceiling. The experimental results showed accurate localization with a root-mean-square error of 0.020 m and a median error of 0.011 m. To determine the limits of the system, accuracy simulations were performed, which confirm the experimental results.**

***Index Terms*— Maximum likelihood estimation (MLE), parameter estimation, position measurement, radio frequency identification (RFID), RFID tags, ultra-high frequency (UHF) technology.**

I. INTRODUCTION

IN RECENT years, radio frequency identification (RFID) has become a key technology in the field of logistics, as it allows identification and tracking of the objects to which the RFID transponders are attached. Since passive tags, which collect the energy from the interrogating electromagnetic field created by RFID readers, can be used, the transponders require no local power source such as batteries. This results in reduced need for maintenance while achieving high flexibility, long lifetime, and low cost. Potential applications would be enhanced considerably if—in addition to identifying RFID tags and thus determining their presence in the interrogation zone of the reader—it were possible to gain reliable information about their accurate position.

In this paper, we present a 2-D position measurement system for passive ultra-high frequency (UHF) RFID transponders based on evaluation of backscattered tag signals. The main application of this system is the localization of stationary objects tagged with RFID labels. A potential use case could be the localization of books in a library. For proof of concept, a local position measurement system demonstrator comprising conventional EPCglobal Class-1 Gen-2 UHF RFID tags, a commercial off-the-shelf RFID reader, eight transceiver frontends, baseband hardware, and signal processing was used for measurements in an indoor office environment. The experimental results confirm that, in terms of accuracy and robustness, the currently popular approaches based on either phase or amplitude evaluation are outperformed by the presented algorithm.

II. RELATED WORK

In contrast to our approach, several systems have been presented which enable localization of mobile devices equipped with RFID readers. If numerous reference RFID tags are distributed at fixed and known locations, the position of the mobile device can be determined by the location of the transponders communicating with the reader [1]–[3]. With this approach, the size of the measurement zone and the system accuracy depend on the way the RFID tags are distributed.

Several systems that allow localization of RFID tags have been introduced in recent years. The method probably used most often derives the estimate of the tag position from the transmission level or the signal strength received by stationary receivers [4]–[6]. Localization systems for passive UHF RFID transponders that build on the k-nearest neighbor principle, where the received signal strength indicator (RSSI) at an RFID reader is compared with the RSSI values of numerous reference tags at fixed and known locations, were introduced in [7] and [8]. Other approaches that require no reference transponders rely on the relationship between received signal strength and distance of the tag from several stationary RFID readers [9], [10]. A probabilistic model for tracking transponders at an RFID gate was described in [11], where a hidden Markov model (HMM) is used to cover both the stochastic nature of read events and the dynamics of a typical identification process within the gate. The HMM is based on

Manuscript received November 14, 2014; revised April 3, 2015; accepted April 6, 2015. This work was supported in part by the Austrian COMET-K2 programme of the Linz Center of Mechatronics, in part by the Austrian Federal Government, and in part by the Federal State of Upper Austria. The Associate Editor coordinating the review process was Dr. Maciej Zawodniok.

M. Scherhäufl and M. Pichler are with the Department of Sensors and Communication, Linz Center of Mechatronics GmbH, Linz 4040, Austria (e-mail: martin.scherhaeufl@lcm.at; markus.pichler@lcm.at).

A. Stelzer is with the Institute for Communications Engineering and RF-Systems, Johannes Kepler University Linz, Linz 4040, Austria (e-mail: a.stelzer@nthfs.jku.at).

Color versions of one or more of the figures in this paper are available online at http://ieeexplore.ieee.org.

Digital Object Identifier 10.1109/TIM.2015.2440554

the RSSI, and with a set of appropriately trained models, it is possible to determine whether a tag is stationary or moving through the RFID gate.

Various RFID localization systems rely on phase evaluation of the tag response signal. Using multiple antenna arrays allows the RFID transponders to be localized based on the angle-of-arrival of the tag response signal or by beam steering [12]–[15]. Since the unwrapped phase-of-arrival (PoA) is proportional to the length of the propagation path, localization of the transponder is enabled by PoA evaluation. However, as there is a 2π ambiguity in phase measurement, systems using a constant carrier frequency require a large number of different signal paths to achieve robust and accurate position estimation [16], [17]. The ambiguity of phase measurement can be handled using several different carrier frequencies, since analysis of the resulting phase differences leads to absolute distance measurements [18]–[21]. However, the performance of these systems depends on the available bandwidth, which is highly constricted by regulatory standards. Several RFID localization systems rely on coherent superposition of phase values sampled by synthetic apertures [22] or inverse synthetic apertures [23]–[25], where movement of either the reader antenna or the RFID transponder is required.

In [26], we have presented a measurement system, where multiple RFID tags must be arranged to form a uniform linear array (ULA). By analyzing the phase of the backscattered transponder signals the presented algorithm estimates the position of the ULA simultaneous with its orientation in azimuth. Using this approach, the ambiguity of phase measurement can be handled by evaluating the phase differences caused by adjacent RFID transponders of the ULA. However, in many cases the required space-intensive tag arrangement cannot be applied to the mobile device. Furthermore, the computational effort of the proposed method is substantial.

In this paper, we present a 2-D localization system for passive UHF RFID transponders based on evaluation of backscattered tag signals. Compared with the system based on a ULA of RFID tags, a similar accuracy is achieved while only single transponders has to be localized, which is more applicable to mobile devices. Furthermore, the computational load is significantly lower since the presented algorithm for localizing the RFID transponders can basically be reduced to matrix multiplications. In contrast to common systems, where either the phase or the amplitude of the received signal is evaluated, combining both parameters offers the advantages of both approaches, leading to accurate and robust localization. Furthermore, the presented algorithm does not rely on reference transponders which are distributed at fixed and known positions, and requires no movement of the reader antenna or the RFID tag for position estimation.

III. System Description

The basic concept of the position measurement system for passive UHF RFID transponders relies on a combination of phase and amplitude evaluation of the received tag signal. If an inventory round is initiated by an RFID reader using one of the K transceiver frontends of the multiple

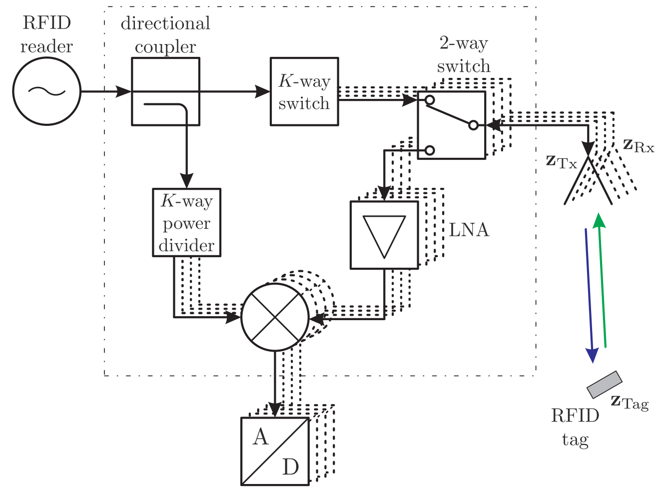

Fig. 1. Schematic of the local position measurement system consisting of K transceiver frontends.

input multiple output (MIMO) system demonstrator, the transponder communicates its information by means of backscatter modulation, where the reflection coefficient of the tag antenna is switched between two stages in accordance with the data being sent. The backscattered tag signal is received by the remaining $K-1$ frontends, amplified by low-noise amplifiers (LNAs), down-converted to baseband, and recorded by analog-to-digital converters. This results in M complex intermediate frequency signals, one for each combination of receiving and transmitting antenna. As both PoA and amplitude of these signals rely on the position of the RFID transponder, localization can be achieved based on each parameter separately. However, due to the combination of phase and amplitude evaluation, the accuracy and the robustness of the position estimates are significantly improved.

IV. Measurement Apparatus

We designed a multiple channel system demonstrator, whose system architecture is shown schematically in Fig. 1. The transmit signal is generated by a commercial off-the-shelf RFID reader configured to use a standardized protocol for identifying the passive UHF RFID tags. This signal feeds to the common port of a K-way switch, which—together with 2-way switches—selects the frontend used for communication between the reader and the tag. The backscattered tag signals occurring at the remaining $K-1$ frontends (configured as receivers) are amplified by LNAs and provide the radio frequency inputs of quadrature demodulators, one for each channel. The local oscillator inputs of these demodulators are supported by a K-way power divider in combination with a directional coupler, which is located in the transmission line. The resulting complex intermediate frequency signals are acquired simultaneously by a multichannel data acquisition card.

V. Signal Model

As presented in [17], the parameters of the intermediate frequency signal occurring at the mth channel of the measurement system are its amplitude $A[m;\boldsymbol{\theta}]$ and PoA $\varphi[m;\boldsymbol{\theta}]$, and

This article has been accepted for inclusion in a future issue of this journal. Content is final as presented, with the exception of pagination.

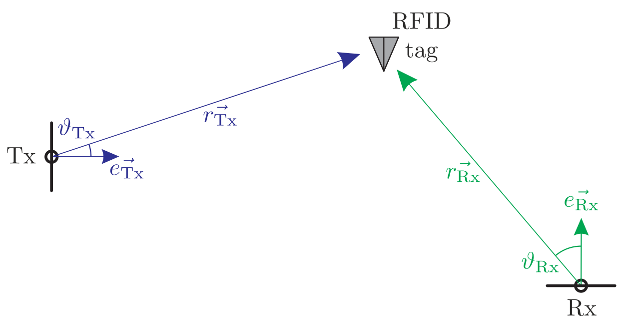

Fig. 2. Schematic of the measurement setup.

can therefore be considered to form a complex vector $\tilde{s}[m;\boldsymbol{\theta}]$

$$\tilde{s}[m;\boldsymbol{\theta}] = A[m;\boldsymbol{\theta}]e^{j\varphi[m;\boldsymbol{\theta}]} \tag{1}$$

where $1 \le m \le M$, and M is the number of channels defined by

$$M = K(K-1) \tag{2}$$

with K representing the number of transceiver frontends of the MIMO system demonstrator. To avoid confusion, we use a tilde to denote a complex quantity. Due to several factors including multipath propagation, cluttering, and environmental conditions, it is assumed that the signal is overlaid with complex noise $\tilde{w}[m]$ with unknown variance σ^2; this leads to the data set

$$\tilde{\mathbf{x}} = \tilde{\mathbf{s}}(\boldsymbol{\theta}) + \tilde{\mathbf{w}}. \tag{3}$$

The parameter vector $\boldsymbol{\theta}$, which has to be determined, specifies the Cartesian coordinates of the position $\mathbf{z}_{\mathrm{Tag}}$ of the mobile RFID transponder

$$\boldsymbol{\theta} = \mathbf{z}_{\mathrm{Tag}} = [x \;\; y]^T. \tag{4}$$

A. Phase-of-Arrival of the Received Transponder Signal

The PoA $\varphi[m;\boldsymbol{\theta}]$ of the received transponder signal depends on the length of the mth propagation path from the transmitting antenna via the RFID tag to the receiving antenna, and therefore contains information about the position $\boldsymbol{\theta}$ of the mobile transponder

$$\varphi[m;\boldsymbol{\theta}] = \frac{2\pi}{\lambda}(|\vec{r_{\mathrm{Tx}}}[m;\boldsymbol{\theta}]| + |\vec{r_{\mathrm{Rx}}}[m;\boldsymbol{\theta}]|) \tag{5}$$

where λ is the wavelength of the transmitted radio frequency signal, and $\vec{r_{\mathrm{Tx}}}[m;\boldsymbol{\theta}]$, $\vec{r_{\mathrm{Rx}}}[m;\boldsymbol{\theta}]$ is the vector pointing from the position of the corresponding antenna of the frontend to the position of the RFID tag

$$\vec{r_{\mathrm{Tx}}}[m;\boldsymbol{\theta}] = \boldsymbol{\theta} - \mathbf{z}_{\mathrm{Tx}}[m] \tag{6}$$

$$\vec{r_{\mathrm{Rx}}}[m;\boldsymbol{\theta}] = \boldsymbol{\theta} - \mathbf{z}_{\mathrm{Rx}}[m]. \tag{7}$$

A schematic of the measurement setup is shown in Fig. 2. Using the first-order Taylor series for linearizing the data set $\tilde{\mathbf{x}}$, the estimates for the PoA $\hat{\boldsymbol{\varphi}}$ can be described by

$$\hat{\boldsymbol{\varphi}} = \angle\tilde{\mathbf{x}} = \boldsymbol{\varphi}(\boldsymbol{\theta}) + \mathbf{w}_{\varphi} \tag{8}$$

where $\mathbf{w}_{\varphi}$ is additive Gaussian noise

$$\mathbf{w}_{\varphi} \sim \mathcal{N}(\boldsymbol{\varphi}_{\mathrm{off}}, \mathbf{C}_{\varphi}) \tag{9}$$

and $\boldsymbol{\varphi}_{\mathrm{off}}$ describes an additional phase offset that depends on various factors including cable length, characteristics of the system demonstrator, and backscatter characteristics of the RFID transponder. The covariance matrix $\mathbf{C}_{\varphi}$ is approximated by a function of the signal amplitude $\hat{\mathbf{A}}$ of the data set

$$\mathbf{C}_{\varphi} = \frac{2\sigma^2}{3}\mathrm{diag}^{-1}(\hat{\mathbf{A}})\;\mathbf{V}_{\varphi}\;\mathrm{diag}^{-1}(\hat{\mathbf{A}}) \tag{10}$$

where $\mathbf{V}_{\varphi}$ is a matrix containing the correlation coefficients between each of the variables in the random vector $\mathbf{w}_{\varphi}$.

B. Amplitude of the Received Transponder Signal

The RFID transponder communicates to the RFID reader by means of backscatter modulation if the energy of the interrogating radio waves exceeds a certain threshold level. However, as described in [7], the reflected signal strength converges in a stable level if the energy of the interrogating radio waves further increases. Therefore, if the RFID transponder is activated by the reader, the amplitude $A[m;\boldsymbol{\theta}]$ impinging at the receiver frontend depends on the length of the mth propagation path from the RFID tag to the receiving antenna and the angle of incidence $\vartheta_{\mathrm{Rx}}[m]$ on the receiving antenna, and therefore contains information about the position $\boldsymbol{\theta}$ of the mobile transponder

$$\begin{aligned} A[m;\boldsymbol{\theta}] &= k_{\mathrm{A}}\frac{\cos(\vartheta_{\mathrm{Rx}}[m;\boldsymbol{\theta}])}{|\vec{r_{\mathrm{Rx}}}[m;\boldsymbol{\theta}]|} \\ &= k_{\mathrm{A}}\frac{\vec{e_{\mathrm{Rx}}}[m]^T\,\vec{r_{\mathrm{Rx}}}[m;\boldsymbol{\theta}]}{|\vec{r_{\mathrm{Rx}}}[m;\boldsymbol{\theta}]|^2} \end{aligned} \tag{11}$$

where $\vec{e_{\mathrm{Rx}}}[m]$ is a unit vector that describes the direction of the main lobe of the receiving antenna, and k_{A} is an unknown but constant factor that is independent of the channel. In detail, this quantity describes various factors including the transmission level of the RFID reader, insertion losses of cables and the system demonstrator, antenna gains, and backscatter characteristics of the RFID transponder. The estimates for the amplitude of the received transponder signal $\hat{\mathbf{A}}$ can be described by

$$\hat{\mathbf{A}} = |\tilde{\mathbf{x}}| = \mathbf{A}(\boldsymbol{\theta}) + \mathbf{w}_{\mathrm{A}}. \tag{12}$$

For common RFID applications, the amplitude of a tag response signal is significantly higher than the noise component. Therefore, although the amplitude cannot be negative, an approximation of the noise $\mathbf{w}_{\mathrm{A}}$ by additive white Gaussian noise (AWGN) can be applied

$$\mathbf{w}_{\mathrm{A}} \sim \mathcal{N}(\mathbf{0}, \mathbf{C}_{\mathrm{A}}). \tag{13}$$

As can be seen in the signal model, the amplitude of the backscattered transponder signal depends only on the receiving path and hence half the sources of interference occur compared with the PoA, which also depends on the transmitting path. Therefore, the variance of the noise component that influences the amplitude is modeled to be half as high compared with the noise component that influences the PoA. The covariance matrix $\mathbf{C}_{\mathrm{A}}$ is therefore defined by

$$\mathbf{C}_{\mathrm{A}} = \frac{\sigma^2}{3}\mathbf{V}_{\mathrm{A}} \tag{14}$$

and $\mathbf{V}_{\mathrm{A}}$ is a matrix containing the correlation coefficients between each of the variables in the random vector $\mathbf{w}_{\mathrm{A}}$.

VI. Localization Method

As previously mentioned, both PoA $\boldsymbol{\varphi}(\boldsymbol{\theta})$ and amplitude $\mathbf{A}(\boldsymbol{\theta})$ of the backscattered transponder signals contain information about the position $\boldsymbol{\theta}$ of the mobile RFID tag, thus allowing localization based on each parameter separately.

A. Phase-of-Arrival-Based Localization

On the basis of the PoA estimates $\hat{\boldsymbol{\varphi}}$ of the backscattered transponder signals, the position of the mobile RFID transponder can be estimated. Since the effect of the additional phase offset $\boldsymbol{\varphi}_{\text{off}}$ can be neglected if the measurement system is calibrated, the signal model for the PoAs $\boldsymbol{\varphi}(\boldsymbol{\theta})$ can be assumed to be influenced by AWGN. In this case, the likelihood function is specified by

$$p_{\varphi}(\tilde{\mathbf{x}};\boldsymbol{\theta}) = \frac{1}{(2\pi)^{\frac{M}{2}}\det^{\frac{1}{2}}(\mathbf{C}_{\varphi})} e^{-\frac{1}{2}(\hat{\boldsymbol{\varphi}}-\boldsymbol{\varphi}(\boldsymbol{\theta}))^T \mathbf{C}_{\varphi}^{-1}(\hat{\boldsymbol{\varphi}}-\boldsymbol{\varphi}(\boldsymbol{\theta}))}. \tag{15}$$

The maximum likelihood estimation (MLE) is defined by the values of $\boldsymbol{\theta}$ that maximize the likelihood function $p_{\varphi}(\tilde{\mathbf{x}};\boldsymbol{\theta})$, which corresponds to the parameters found by minimizing the cost function

$$J_{\varphi}(\tilde{\mathbf{x}};\boldsymbol{\theta}) = \frac{1}{2}(\hat{\boldsymbol{\varphi}}-\boldsymbol{\varphi}(\boldsymbol{\theta}))^T \mathbf{C}_{\varphi}^{-1}(\hat{\boldsymbol{\varphi}}-\boldsymbol{\varphi}(\boldsymbol{\theta})). \tag{16}$$

Since uncorrelated noise ($\mathbf{V}_{\varphi} = \mathbf{I}$) is assumed when finding the MLE, the cost function can be expressed by

$$J_{\varphi}(\tilde{\mathbf{x}};\boldsymbol{\theta}) = \frac{3}{4\sigma^2}(\hat{\boldsymbol{\varphi}}-\boldsymbol{\varphi}(\boldsymbol{\theta}))^T \operatorname{diag}^2(\hat{\mathbf{A}})(\hat{\boldsymbol{\varphi}}-\boldsymbol{\varphi}(\boldsymbol{\theta})). \tag{17}$$

Hence, the parameters $\boldsymbol{\theta}$ can be estimated as the values that minimize the function

$$(\hat{\boldsymbol{\varphi}}-\boldsymbol{\varphi}(\boldsymbol{\theta}))^T \operatorname{diag}^2(\hat{\mathbf{A}})(\hat{\boldsymbol{\varphi}}-\boldsymbol{\varphi}(\boldsymbol{\theta})) \tag{18}$$

where the PoAs must be wrapped such that the phase difference is within the interval $[-\pi, \pi]$. Finding the MLE is therefore a nonlinear problem. Since analytic algorithms for finding an optimum are not yet known and the convergence of iterative algorithms cannot be guaranteed due to phase ambiguity, we propose the application of a numerical grid search approach.

A significant reduction in computational effort can be achieved if we allow an approximation of (18). To this end, we introduce a utility function

$$\begin{aligned} P_{\varphi}(\tilde{\mathbf{x}};\boldsymbol{\theta}) &= \operatorname{Re}\left((e^{j\hat{\boldsymbol{\varphi}}})^H \operatorname{diag}^2(\hat{\mathbf{A}}) e^{j\boldsymbol{\varphi}(\boldsymbol{\theta})}\right) \\ &= \sum_{m=1}^{M} \hat{A}[m]^2 \cos(\hat{\varphi}[m] - \varphi[m;\boldsymbol{\theta}]) \end{aligned} \tag{19}$$

which can basically be calculated by a matrix multiplication. Furthermore, wrapping the phase differences in order for them to fall within the interval $[-\pi, \pi]$ is no longer necessary. Using the second-order Taylor series for the cosine function, the utility function can be approximated by

$$P_{\varphi}(\tilde{\mathbf{x}};\boldsymbol{\theta}) \approx \hat{\mathbf{A}}^T\hat{\mathbf{A}} - \frac{1}{2}(\hat{\boldsymbol{\varphi}}-\boldsymbol{\varphi}(\boldsymbol{\theta}))^T \operatorname{diag}^2(\hat{\mathbf{A}})(\hat{\boldsymbol{\varphi}}-\boldsymbol{\varphi}(\boldsymbol{\theta})) \tag{20}$$

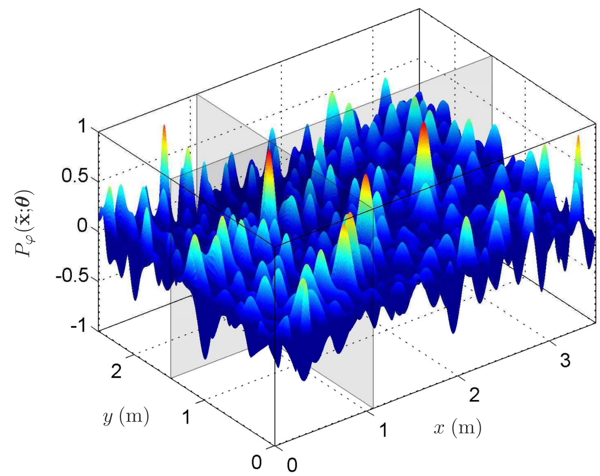

Fig. 3. Utility function $P_{\varphi}(\tilde{\mathbf{x}};\boldsymbol{\theta})$ used for localization of passive UHF RFID transponders based on phase evaluation. The measurements were carried out in an indoor office environment using $K = 8$ transceiver frontends.

where the second term is a negative and scaled version of the cost function, which results in

$$J_{\varphi}(\tilde{\mathbf{x}};\boldsymbol{\theta}) \approx \frac{3}{2\sigma^2}\Big(\hat{\mathbf{A}}^T\hat{\mathbf{A}} - \underbrace{\operatorname{Re}\left((e^{j\hat{\boldsymbol{\varphi}}})^H \operatorname{diag}^2(\hat{\mathbf{A}}) e^{j\boldsymbol{\varphi}(\boldsymbol{\theta})}\right)}_{P_{\varphi}(\tilde{\mathbf{x}};\boldsymbol{\theta})}\Big). \tag{21}$$

Since the term $\hat{\mathbf{A}}^T\hat{\mathbf{A}}$ is not influenced by $\boldsymbol{\theta}$ and thus irrelevant to parameter estimation, minimizing the cost function $J_{\varphi}(\tilde{\mathbf{x}};\boldsymbol{\theta})$ is equivalent to maximizing the utility function $P_{\varphi}(\tilde{\mathbf{x}};\boldsymbol{\theta})$. Hence, an approximation of the MLE can be found by

$$\hat{\boldsymbol{\theta}}_{\varphi} = \arg\max_{\boldsymbol{\theta}} \left(\operatorname{Re}\left((e^{j\hat{\boldsymbol{\varphi}}})^H \operatorname{diag}^2(\hat{\mathbf{A}}) e^{j\boldsymbol{\varphi}(\boldsymbol{\theta})}\right)\right). \tag{22}$$

In the majority of cases, localization of passive UHF RFID transponders by means of PoA evaluation leads to accurate position estimates. However, outliers can occur due to 2π phase ambiguity. The utility function $P_{\varphi}(\tilde{\mathbf{x}};\boldsymbol{\theta})$ of the estimator based on PoA evaluation is shown in Fig. 3. As can be seen, there are several high peaks, of which the highlighted one shows the highest value for $P_{\varphi}(\tilde{\mathbf{x}};\boldsymbol{\theta})$ but belongs to an incorrect position estimate.

B. Amplitude-Based Localization

Localization of the passive UHF RFID tags can be achieved by evaluating the amplitude estimates $\hat{\mathbf{A}}$ of the backscattered transponder signals. Since it is assumed that the amplitude values are covered by AWGN, the likelihood function can be defined by

$$p_{\mathrm{A}}(\tilde{\mathbf{x}};\boldsymbol{\theta}) = \frac{1}{(2\pi)^{\frac{M}{2}}\det^{\frac{1}{2}}(\mathbf{C}_{\mathrm{A}})} e^{-\frac{1}{2}(\hat{\mathbf{A}}-\mathbf{A}(\boldsymbol{\theta}))^T \mathbf{C}_{\mathrm{A}}^{-1}(\hat{\mathbf{A}}-\mathbf{A}(\boldsymbol{\theta}))}. \tag{23}$$

The MLE of $\boldsymbol{\theta}$ are the values that maximize the likelihood function $p_{\mathrm{A}}(\tilde{\mathbf{x}};\boldsymbol{\theta})$ or, equivalently, the values that minimize the cost function

$$J_{\mathrm{A}}(\tilde{\mathbf{x}};\boldsymbol{\theta}) = \frac{1}{2}(\hat{\mathbf{A}}-\mathbf{A}(\boldsymbol{\theta}))^T \mathbf{C}_{\mathrm{A}}^{-1}(\hat{\mathbf{A}}-\mathbf{A}(\boldsymbol{\theta})). \tag{24}$$

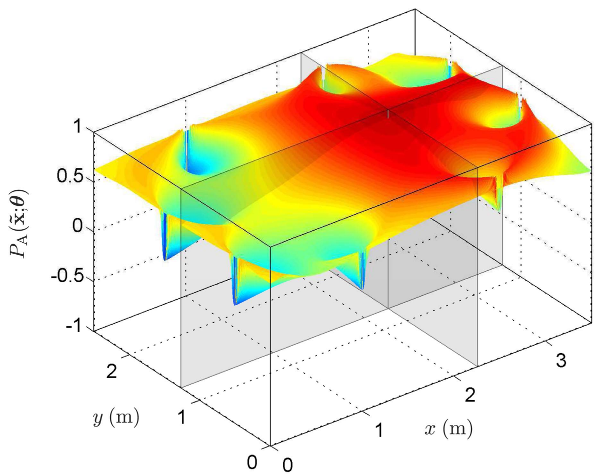

Fig. 4. Utility function $P_\mathrm{A}(\tilde{\mathbf{x}}; \boldsymbol{\theta})$ used for localization of passive UHF RFID transponders based on amplitude evaluation. The measurements were carried out in an indoor office environment using $K = 8$ transceiver frontends.

Because uncorrelated noise ($\mathbf{V}_\mathrm{A} = \mathbf{I}$) is assumed when finding the MLE, the cost function can be expressed by

$$J_\mathrm{A}(\tilde{\mathbf{x}}; \boldsymbol{\theta}) = \frac{3}{2\sigma^2}(\hat{\mathbf{A}} - \mathbf{A}(\boldsymbol{\theta}))^T(\hat{\mathbf{A}} - \mathbf{A}(\boldsymbol{\theta})). \tag{25}$$

Since the signal model for the amplitudes $\mathbf{A}(\boldsymbol{\theta})$ of the backscattered transponder signals includes an unknown but constant factor k_A, an immediate minimization of this function can hardly be achieved. However, the cost function can be expanded to

$$J_\mathrm{A}(\tilde{\mathbf{x}}; \boldsymbol{\theta}) = \frac{3}{2\sigma^2}(\hat{\mathbf{A}}^T\hat{\mathbf{A}} - 2\hat{\mathbf{A}}^T\mathbf{A}(\boldsymbol{\theta}) + \mathbf{A}(\boldsymbol{\theta})^T\mathbf{A}(\boldsymbol{\theta})). \tag{26}$$

If the signals are normalized such that

$$\hat{\mathbf{A}}^T\hat{\mathbf{A}} = 1 \tag{27}$$

$$\mathbf{A}(\boldsymbol{\theta})^T\mathbf{A}(\boldsymbol{\theta}) = 1 \tag{28}$$

the unknown factor k_A can be neglected and the cost function results in

$$J_\mathrm{A}(\tilde{\mathbf{x}}; \boldsymbol{\theta}) = \frac{3}{\sigma^2}(1 - \hat{\mathbf{A}}^T\mathbf{A}(\boldsymbol{\theta})). \tag{29}$$

As minimizing the cost function $J_\mathrm{A}(\tilde{\mathbf{x}}; \boldsymbol{\theta})$ is equivalent to maximizing the utility function

$$P_\mathrm{A}(\tilde{\mathbf{x}}; \boldsymbol{\theta}) = \hat{\mathbf{A}}^T\mathbf{A}(\boldsymbol{\theta}) \tag{30}$$

the MLE of the parameters $\boldsymbol{\theta}$ is found by

$$\hat{\boldsymbol{\theta}}_\mathrm{A} = \arg\max_{\boldsymbol{\theta}}(\hat{\mathbf{A}}^T\mathbf{A}(\boldsymbol{\theta})). \tag{31}$$

The most likely values for $\boldsymbol{\theta}$ can be found by a numerical grid search approach, where normalization of the theoretical values of the amplitudes $\mathbf{A}(\boldsymbol{\theta})$ must be performed for each discrete position according to (28). Localization of passive UHF RFID transponders by means of amplitude evaluation leads to robust position estimates. However, the accuracy of the algorithm is not sufficient in the majority of cases. The utility function $P_\mathrm{A}(\tilde{\mathbf{x}}; \boldsymbol{\theta})$ of the estimator based on amplitude evaluation is shown in Fig. 4. As can be seen, the process of finding the maximum value for $P_\mathrm{A}(\tilde{\mathbf{x}}; \boldsymbol{\theta})$ can be inaccurate due to the flat curve progression.

C. Localization Based on Received Transponder Signals

As previously mentioned, localization of passive UHF RFID transponders based on PoA evaluation offers excellent accuracy in the majority of cases, but several outliers occur due to phase ambiguity. Conversely, localization by means of amplitude evaluation exhibits good robustness but less accuracy. The advantages of both algorithms can be combined if both parameters $\hat{\boldsymbol{\varphi}}$ and $\hat{\mathbf{A}}$ of the received transponder signals are evaluated. To this end, a joint likelihood function is introduced with

$$p(\tilde{\mathbf{x}}; \boldsymbol{\theta}) = p_\varphi(\tilde{\mathbf{x}}; \boldsymbol{\theta})\, p_\mathrm{A}(\tilde{\mathbf{x}}; \boldsymbol{\theta}). \tag{32}$$

The MLE is defined by the values of $\boldsymbol{\theta}$ which maximize the joint likelihood function $p(\tilde{\mathbf{x}}; \boldsymbol{\theta})$. Since a multiplication of the exponential functions $p_\varphi(\tilde{\mathbf{x}}; \boldsymbol{\theta})$ and $p_\mathrm{A}(\tilde{\mathbf{x}}; \boldsymbol{\theta})$ leads to an addition of their exponents which were defined as the negative versions of the cost functions $J_\varphi(\tilde{\mathbf{x}}; \boldsymbol{\theta})$ and $J_\mathrm{A}(\tilde{\mathbf{x}}; \boldsymbol{\theta})$, the MLE can equivalently be defined as the parameters that minimize the joint cost function

$$J(\tilde{\mathbf{x}}; \boldsymbol{\theta}) = J_\varphi(\tilde{\mathbf{x}}; \boldsymbol{\theta}) + J_\mathrm{A}(\tilde{\mathbf{x}}; \boldsymbol{\theta}). \tag{33}$$

Using the definitions (21), (27), and (29), the joint cost function can be expressed by

$$\begin{aligned} J(\tilde{\mathbf{x}}; \boldsymbol{\theta}) = {} & \frac{3}{2\sigma^2}\left(1 - \mathrm{Re}\left((e^{j\hat{\boldsymbol{\varphi}}})^H \mathrm{diag}^2(\hat{\mathbf{A}}) e^{j\boldsymbol{\varphi}(\boldsymbol{\theta})}\right)\right) \\ & + \frac{3}{\sigma^2}(1 - \hat{\mathbf{A}}^T\mathbf{A}(\boldsymbol{\theta})). \end{aligned} \tag{34}$$

As minimizing the cost function $J(\tilde{\mathbf{x}}; \boldsymbol{\theta})$ is equivalent to maximizing the utility function

$$P(\tilde{\mathbf{x}}; \boldsymbol{\theta}) = \mathrm{Re}\left((e^{j\hat{\boldsymbol{\varphi}}})^H \mathrm{diag}^2(\hat{\mathbf{A}}) e^{j\boldsymbol{\varphi}(\boldsymbol{\theta})}\right) + 2\hat{\mathbf{A}}^T\mathbf{A}(\boldsymbol{\theta}) \tag{35}$$

the MLE of the parameters $\boldsymbol{\theta}$ is found by

$$\hat{\boldsymbol{\theta}} = \arg\max_{\boldsymbol{\theta}}\left(\mathrm{Re}((e^{j\hat{\boldsymbol{\varphi}}})^H \mathrm{diag}^2(\hat{\mathbf{A}}) e^{j\boldsymbol{\varphi}(\boldsymbol{\theta})}) + 2\hat{\mathbf{A}}^T\mathbf{A}(\boldsymbol{\theta})\right). \tag{36}$$

Again, the most likely values for $\boldsymbol{\theta}$ can be found by a numerical grid search approach. The utility function $P(\tilde{\mathbf{x}}; \boldsymbol{\theta})$ of the estimator based on evaluation of both parameters of the received transponder signals can be observed in Fig. 5. As can be seen, similar to the results of the algorithm based on PoA evaluation several peaks arise due to phase ambiguity. However, due to the combination with amplitude evaluation, peaks at incorrect positions are reduced in their amplitude. Therefore, outliers due to phase ambiguity are avoided while the accuracy of the positions estimates remains almost unchanged compared with the algorithm based on PoA evaluation. This leads in contrast to Fig. 3 to an accurate position estimate using the same data set.

VII. Simulation Results

Simulations using the Monte Carlo method were carried out to evaluate the performance of the position estimators specified by (22), (31), and (36). To this end, a 2-D localization system using $K = 8$ transceiver frontends and a measurement zone defined by 3.5 m × 2.5 m was simulated, and the data set was overlaid with complex noise as described by (3). Since the main disturbance occurring at a given channel is due

This article has been accepted for inclusion in a future issue of this journal. Content is final as presented, with the exception of pagination.

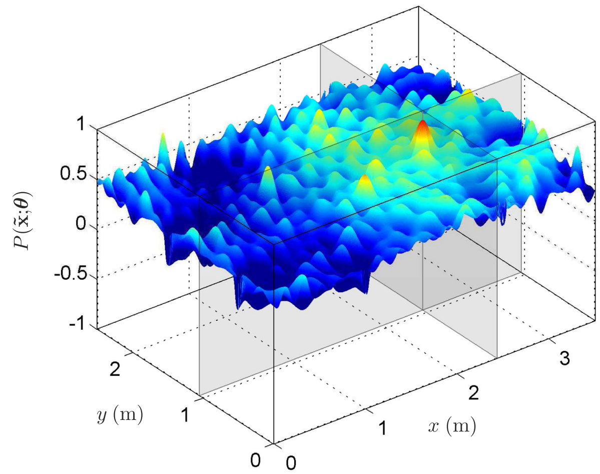

Fig. 5. Utility function $P(\tilde{\mathbf{x}};\boldsymbol{\theta})$ used for localization of passive UHF RFID tags based on evaluation of the received transponder signals. The measurements were carried out in an indoor office environment using $K = 8$ transceiver frontends.

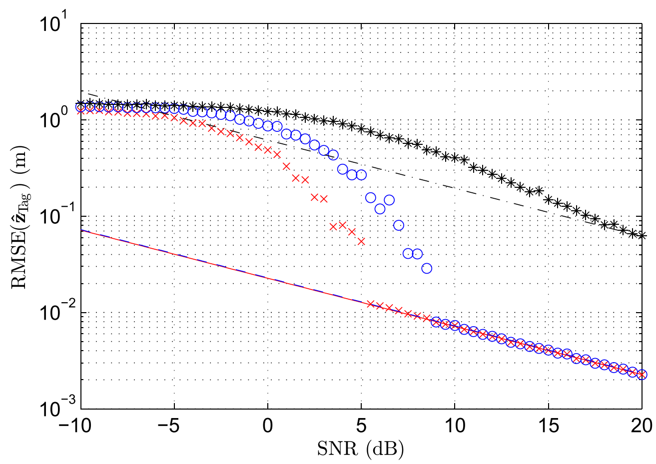

Fig. 6. Simulation of the accuracy of the position estimator using the Monte Carlo method. Phase evaluation: _ _ CRLB, ○ simulated RMSE. Amplitude evaluation: _ . _ CRLB, $*$ simulated RMSE. Combined evaluation: ___ CRLB, × simulated RMSE.

to multipath propagation, which is assumed to be constant during a measurement cycle, the noise was considered to be correlated for individual measurements. The simulation was performed a thousand times, and then a different signal-to-noise ratio (SNR) was chosen. The analytically calculated Cramér–Rao lower bound (CRLB), which states the minimum variance that can be achieved by an unbiased estimator, was used as a benchmark with which the performance of the estimator was compared. As shown in Fig. 6, the root-mean-square error (RMSE) of the position estimates depends on the SNR. As a result of the limited size of the measurement zone, the RMSE cannot exceed a certain threshold level even at low SNR. As can be seen, the estimator based on amplitude evaluation offers the lowest accuracy of all approaches and is therefore used only as a component of the estimator based on combined phase and amplitude evaluation. At an SNR threshold level of approximately 5.5 dB, the estimator based on the combination of both parameters of the received

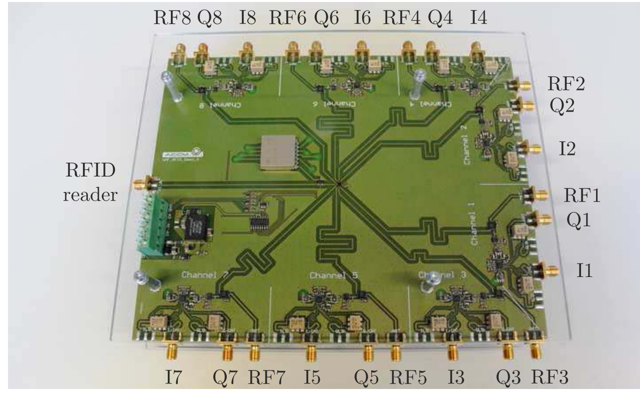

Fig. 7. System demonstrator designed to support $K = 8$ transceiver frontends. RF# is the antenna port, and I# and Q# are the outputs of the demodulator for in-phase and quadrature, respectively.

transponder signal starts to asymptotically approach the corresponding CRLB. This is a significant improvement compared with the estimator based on phase evaluation, in which the almost identical CRLB is not approached until a threshold of approximately 9 dB is exceeded.

VIII. Measurement Results

To evaluate the performance of the localization system, measurements were carried out in an indoor office environment which was surrounded by drywalls and a concrete floor and ceiling. To this end, a local position measurement system demonstrator consisting of $K = 8$ transceiver frontends was built, resulting in $M = 56$ channels of the measurement system. The system demonstrator is shown in Fig. 7.

The corresponding linearly polarized antennas were distributed at a height of 1.6 m above the floor at the border of the 2-D measurement zone, which was defined as 3.5 m × 2.5 m. An EPCglobal Class-1 Gen-2/ISO 18000-6C compliant UHF RFID reader was used to communicate with a linearly polarized passive UHF RFID transponder, which was attached to a 2-D traversing rail by means of a plastic tube. The transponder was moved to 645 defined positions located in the transceive antenna plane; the actual positions were only used to verify system accuracy and did not affect the localization algorithms.

The RFID reader was configured to generate a transmit single using a carrier frequency of 866.9 MHz and a signal level of 2 W equivalent radiated power. As can be seen in Fig. 8, a strong line-of-sight propagation was present in this scenario. However, several static reflections and multipath propagation generated by drywalls, concrete floor, and ceiling were expected.

As previously mentioned, calibration is necessary to enable localization by means of phase evaluation. To this end, reference measurements using 10 known transponder positions were carried out, where a comparison between measured and calculated PoA values led to estimates of the phase offset $\boldsymbol{\varphi}_{\mathrm{off}}$ according to (9).

A. Phase-of-Arrival-Based Localization

Localization of passive UHF RFID tags can be achieved by applying the algorithm specified by (22), where the PoAs $\hat{\boldsymbol{\varphi}}$

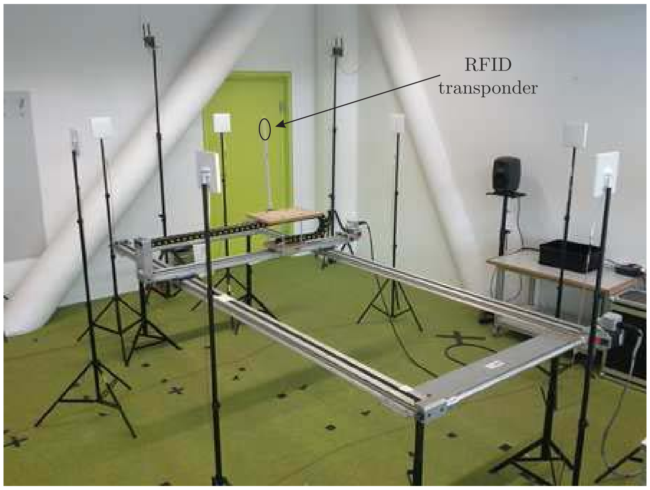

Fig. 8. Measurement setup of the localization system for passive UHF RFID transponders consisting of $K = 8$ transceiver frontends.

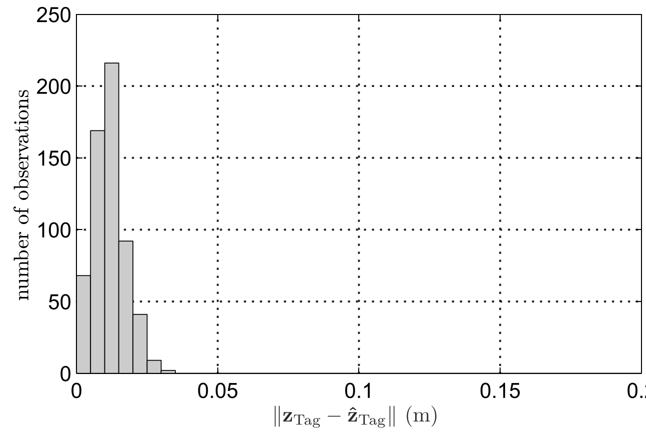

Fig. 10. Distribution of the absolute error of the position estimates based on 645 measurements carried out in an indoor office environment, evaluating the PoAs of the received transponder signals. 48 measurements showed an error of more than 0.2 m.

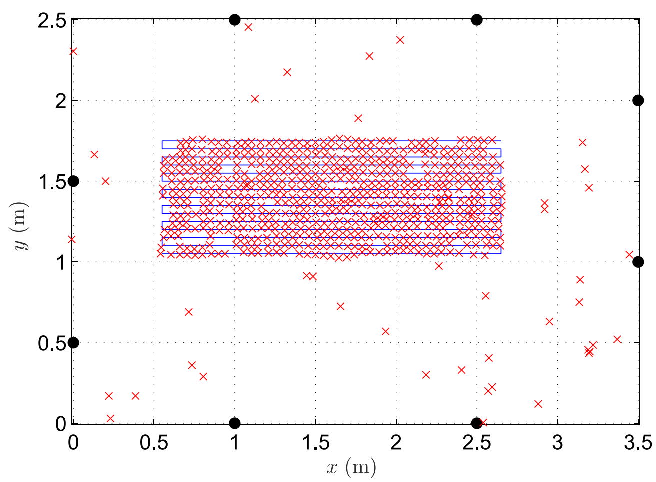

Fig. 9. Localization of passive UHF RFID transponders based on phase evaluation; ● antenna position, — actual track of the RFID tag, and × estimated transponder position.

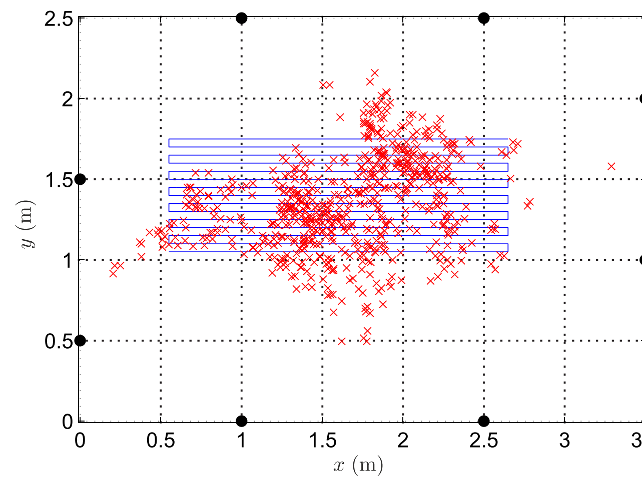

Fig. 11. Localization of passive UHF RFID transponders based on amplitude evaluation; ● antenna position, — actual track of the RFID tag, and × estimated transponder position.

of the received transponder signals are evaluated. The median error and the RMSE of the position estimates were calculated as 0.011 and 0.47 m, respectively. Since the measurements showed an SNR of approximately 5.75 dB, which is significantly lower than the threshold of 9 dB determined by Monte Carlo simulations using this algorithm, outliers of the position estimates occur due to unwrapping problems, which explain the huge difference between the median error and the RMSE. As can be seen in Figs. 9 and 10, localization of passive UHF RFID transponders based on phase evaluation is accurate in the majority of cases. Specifically, 92.6% of the tag positions were estimated with an error below 0.04 m. However, due to the outliers, the maximum absolute error of the position estimates was evaluated to be 2.97 m.

B. Amplitude-Based Localization

The positions of the passive UHF RFID transponders can be estimated based on the algorithm specified by (31), evaluating the signal strength of the received transponder signals. With this algorithm the median error increases to 0.26 m, but the RMSE decreases to 0.35 m. As shown in Figs. 11 and 12, this algorithm is relatively inaccurate. However, as this algorithm is not affected by unwrapping problems, the maximum absolute error of the position estimates was evaluated to be 1.29 m, which is a significant improvement compared with the algorithm based on phase evaluation.

C. Localization Based on Received Transponder Signal

As described before, due to the combination of phase and amplitude evaluation, an improvement in accuracy and robustness of the position estimates is expected. If the algorithm specified by (36) is used for localization of passive UHF RFID tags, the RMSE indeed decreases to 0.020 m, while the median error remains unchanged at 0.011 m compared with phase evaluation. As can be observed in Figs. 13 and 14, the position estimation is accurate in the majority of cases. In detail, only one outlier with an absolute error of 0.40 m occurred, while the remaining position estimates showed an error below 0.04 m. In general, outliers can be explained by the fact that the measurements showed an SNR of

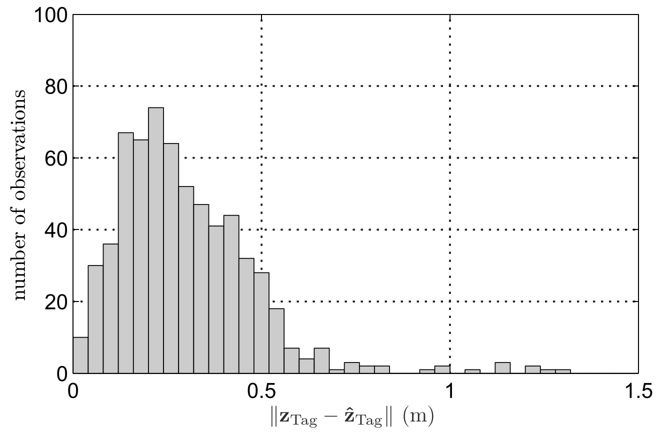

Fig. 12. Distribution of the absolute error of the position estimates based on 645 measurements carried out in an indoor office environment, evaluating the amplitudes of the received transponder signals.

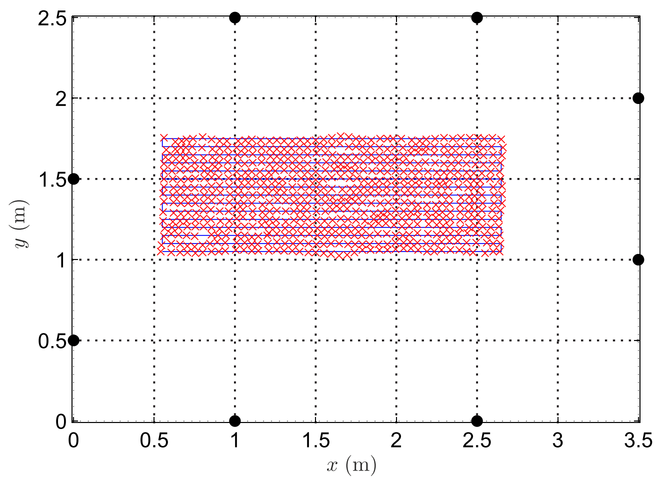

Fig. 13. Localization of passive UHF RFID transponders based on evaluation of both received transponder signal parameters $\hat{\boldsymbol{\varphi}}$ and $\hat{\mathbf{A}}$; ● antenna position, — actual track of the RFID tag, and × estimated transponder position.

approximately 5.75 dB, which is close to the threshold level of 5.5 dB determined by Monte Carlo simulations. Furthermore, the localization performance is degraded if some tag/front-end combinations do not produce a tag response. For an SNR of 5.75 dB, the CRLB yields a standard deviation of the unbiased estimator of 0.012 m, which is close to the RMSE of 0.020 m obtained by the measurements. To prove the performance of the proposed method, further measurements have been performed using an SNR below the threshold level of 5.5 dB. To this end, several stationary reflectors were added to the measurement scenario. The experiments showed that at an SNR of 4.10 dB the RMSE of the position estimates increases to 0.084 m. This value is very similar compared with the results determined by Monte Carlo simulations, which would lead to an RMSE of 0.079 m.

A strategy to avoid outliers would be to increase the number of transceiver frontends, since this would reduce the SNR required to achieve robust position estimates. Alternatively, by increasing the transmission power or by reducing the insertion loss of the system demonstrator, the number of tag responses could be increased, which would improve localization accuracy and robustness.

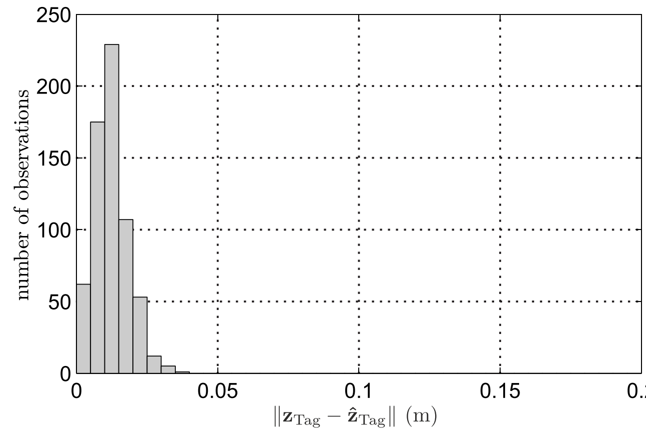

Fig. 14. Distribution of the absolute error of the position estimates based on 645 measurements carried out in an indoor office environment in which both received transponder signal parameters $\hat{\boldsymbol{\varphi}}$ and $\hat{\mathbf{A}}$ were evaluated. One measurement showed an error of more than 0.2 m.

In general, the computational effort of methods using a numerical grid search approach can be substantial. Obviously, the grid density has to be chosen as a tradeoff between accuracy and computational load. Algorithms based on PoA evaluation require a grid with a spacing significantly smaller than the wavelength, which leads to a large number of discrete positions and therefore to a high computational load. However, since the theoretical values of the parameters PoA $\boldsymbol{\varphi}(\boldsymbol{\theta})$ and amplitude $\mathbf{A}(\boldsymbol{\theta})$ can be calculated in advance for each discrete position of the grid and since the algorithms for localizing the RFID transponders can be reduced to matrix multiplications, even using a grid spacing of 1 cm, the time required for calculating the position estimates can be neglected compared with the time the system takes to sequentially configure each frontend as transmitter and perform an inventory round by means of the RFID reader.

D. Comparison of Localization Methods

A comparison of different localization schemes that provide experimental results is given in Table I. In contrast to our approach, the analyzed methods of localizing mobile RFID readers rely on numerous stationary reference transponders at fixed and known positions, where the localization accuracy depends on the density of the tags [1], [2]. A remarkable benefit of these approaches is that the measurement zone is restricted only by the arrangement of the transponders.

Since the analyzed systems that allow localization of passive UHF RFID tags are based on evaluation of the backscattered transponder signal, their measurement zones are always limited by the read range. If reference transponders at fixed and known positions are used to enable position estimation, localization can be achieved by RSSI evaluation at a stationary RFID reader [7], [8]. These systems show moderate localization accuracy, which depends on the number of reference transponders distributed in the measurement zone.

If the transponder signals received at several reader antennas are evaluated, localization can be achieved without the use of reference tags. Similar to the algorithm for amplitude-based localization presented in this paper, the method introduced in [10] allows localization of passive UHF RFID tags by

This article has been accepted for inclusion in a future issue of this journal. Content is final as presented, with the exception of pagination.

TABLE I
COMPARISON OF LOCALIZATION METHODS

Reference	Target	Approach	Average Accuracy	Measurement Zone	Note
Errington *et al.* [1]	Reader	RSSI	20.5 cm	N/A	Reference transponders at known positions required; localization accuracy depends on density of RFID tags
Shirehjini *et al.* [2]	Reader	RSSI	6.5 cm	N/A	Reference transponders at known positions required; localization accuracy depends on density of RFID tags
Chen *et al.* [7]	Tag	RSSI	31 cm	3.1 m x 1.2 m	Reference transponders at known positions required; localization of the RFID tags based on the k-nearest neighbor principle
Zhang *et al.* [8]	Tag	RSSI	18 cm	4.2 m x 2.8 m	Reference transponders at known positions required; localization of the RFID tags based on the k-nearest neighbor principle
Shao *et al.* [10]	Tag	RSSI	35.4 cm	3 m x 2 m	Evaluation of the received signal strength of 4 reader antennas
Azzouzi *et al.* [14]	Tag	PoA	10.7 cm	3 m x 3 m	Evaluation of the angle-of-arrival of the received signal at 5 antenna arrays
Scherhäufl *et al.* [17]	Tag	PoA	56 cm	3.5 m x 2.5 m	MIMO system consisting of 8 frontends; system calibration is required
Povalac *et al.* [20]	Tag	PoA	14 cm	$\leq$ 2.5 m (1-D)	Phase evaluation using different carrier frequencies; system calibration is required
Miesen *et al.* [22]	Tag	PoA	2 cm (lateral); 90 cm (distance)	N/A	Synthetic aperture created by moving reader antenna at known trajectory
Scherhäufl *et al.* [23]	Tag	PoA	6.4 cm	3.5 m x 2.5 m	Inverse synthetic aperture created by moving tag; system calibration is required
Parr *et al.* [24]	Tag	PoA	1 cm (lateral); 5 cm (distance)	N/A	Inverse synthetic aperture created by moving tag at known trajectory
Scherhäufl *et al.* [26]	ULA	PoA	1.1 cm	3.5 m x 2.5 m	Localization of a ULA of 6 RFID transponders; MIMO system consisting of 8 frontends; system calibration is required
This work	Tag	PoA + RSSI	2.0 cm	3.5 m x 2.5 m	MIMO system consisting of 8 frontends; evaluation of backscattered transponder signals; system calibration is required

evaluating the RSSI values provided by four commercial RFID readers.

In general, systems using phase evaluation show better accuracy than systems using RSSI evaluation. By evaluating the angle-of-arrival of the received transponder signal at several antenna arrays that are placed at the edge of the 2-D measurement zone, a method to localize RFID tags was introduced in [14]. This system offers accurate localization at the price of using user-defined antenna arrays. In [17], we introduced an approach enabling transponder localization based on analyzing the PoA using numerous transceiver frontends. Since this algorithm is related to the method of localizing RFID tags by means of phase evaluation presented in this paper, similar results are achieved. Analyzing the phase differences using various carrier frequencies enables position estimation by the method presented in [20], where the localization performance depends on the available bandwidth, which is limited by regulatory standards.

Several systems have been analyzed which are based on coherent superposition of phase values sampled by synthetic apertures [22] or inverse synthetic apertures [23], [24]. These systems offer high accuracy, but in contrast to our work a localization of stationary RFID transponders cannot be achieved as these systems require movement of either the reader antenna or the RFID tags.

In [26], we proposed a method of localizing a ULA of RFID transponders based on phase evaluation. The experiments, which were performed using the same system demonstrator as and a measurement setup similar to that described in this paper showed excellent accuracy and robustness. However, in many cases the required space-intensive tag arrangement cannot be applied to the mobile device. Furthermore, the computational effort is significantly higher compared with the approach presented in this paper.

In summary, as each method has its own shortcomings, no system could be found that offers optimum characteristics for all cases. The system introduced in this paper exhibits the highest accuracy of all investigated methods for the most common case, where only a single RFID transponder must be localized and movement of either the reader antenna or the RFID tag along a known trajectory cannot be guaranteed. Furthermore, in contrast to various other methods, no reference transponders are necessary to allow position estimation. However, like most approaches that evaluate the PoA of the received transponder signal, system calibration is required for localization.

IX. CONCLUSION

We have introduced a 2-D localization system for passive UHF RFID tags based on evaluation of backscattered transponder signals. In contrast to a variety of common systems, where either the phase or the amplitude of the received transponder signal is evaluated, our method of incorporating both parameters combines the advantages of both approaches. Furthermore, the presented algorithm does not rely on reference transponders, and no movement of the reader antenna or the RFID tag is necessary to allow position estimation. The system, which combines eight transceiver frontends, uses a commercial off-the-shelf RFID reader and conventional passive EPCglobal Class-1 Gen-2 UHF RFID transponders. Measurements performed by means of a system demonstrator in an indoor office environment surrounded by drywalls and concrete floor and ceiling showed accurate and robust localization while meeting the regulatory standards.

REFERENCES

[1] A. F. C. Errington, B. L. F. Daku, and A. F. Prugger, "Initial position estimation using RFID tags: A least-squares approach," *IEEE Trans. Instrum. Meas.*, vol. 59, no. 11, pp. 2863–2869, Nov. 2010.

[2] A. A. N. Shirehjini, A. Yassine, and S. Shirmohammadi, "An RFID-based position and orientation measurement system for mobile objects in intelligent environments," *IEEE Trans. Instrum. Meas.*, vol. 61, no. 6, pp. 1664–1675, Jun. 2012.

[3] J. H. Cho and M.-W. Cho, "Effective position tracking using B-spline surface equation based on wireless sensor networks and passive UHF-RFID," *IEEE Trans. Instrum. Meas.*, vol. 62, no. 9, pp. 2456–2464, Sep. 2013.

[4] A. Athalye, V. Savic, M. Bolic, and P. M. Djuric, "Novel semi-passive RFID system for indoor localization," *IEEE Sensors J.*, vol. 13, no. 2, pp. 528–537, Feb. 2013.

[5] A. Dionisi, E. Sardini, and M. Serpelloni, "Wearable object detection system for the blind," in *Proc. IEEE Int. Instrum. Meas. Technol. Conf. (I2MTC)*, May 2012, pp. 1255–1258.

[6] B. Jachimczyk, D. Dziak, and W. J. Kulesza, "RFID—Hybrid scene analysis-neural network system for 3D indoor positioning optimal system arrangement approach," in *Proc. IEEE Int. Instrum. Meas. Technol. Conf. (I2MTC)*, May 2014, pp. 191–196.

[7] X. Chen, L. Xie, C. Wang, and S. Lu, "Adaptive accurate indoor-localization using passive RFID," in *Proc. IEEE Int. Conf. Parallel Distrib. Syst. (ICPADS)*, Dec. 2013, pp. 249–256.

[8] Z. Zhang, Z. Lu, V. Saakian, X. Qin, Q. Chen, and L.-R. Zheng, "Item-level indoor localization with passive UHF RFID based on tag interaction analysis," *IEEE Trans. Ind. Electron.*, vol. 61, no. 4, pp. 2122–2135, Apr. 2014.

[9] A. R. J. Ruiz, F. S. Granja, J. C. P. Honorato, and J. I. G. Rosas, "Accurate pedestrian indoor navigation by tightly coupling foot-mounted IMU and RFID measurements," *IEEE Trans. Instrum. Meas.*, vol. 61, no. 1, pp. 178–189, Jan. 2012.

[10] S. Shao and R. J. Burkholder, "Item-level RFID tag location sensing utilizing reader antenna spatial diversity," *IEEE Sensors J.*, vol. 13, no. 10, pp. 3767–3774, Oct. 2013.

[11] M. Goller and M. Brandner, "Improving classification performance of RFID gates using hidden Markov models," in *Proc. IEEE Int. Instrum. Meas. Technol. Conf. (I2MTC)*, May 2011, pp. 1–5.

[12] C. Hekimian-Williams, B. Grant, X. Liu, Z. Zhang, and P. Kumar, "Accurate localization of RFID tags using phase difference," in *Proc. IEEE Int. Conf. RFID*, Apr. 2010, pp. 89–96.

[13] J. Zhou, H. Zhang, and L. Mo, "Two-dimension localization of passive RFID tags using AOA estimation," in *Proc. IEEE Int. Instrum. Meas. Technol. Conf. (I2MTC)*, May 2011, pp. 1–5.

[14] S. Azzouzi, M. Cremer, U. Dettmar, T. Knie, and R. Kronberger, "Improved AoA based localization of UHF RFID tags using spatial diversity," in *Proc. IEEE Int. Conf. RFID-Technol. Appl. (RFID-TA)*, Sep. 2011, pp. 174–180.

[15] N. Guzey, H. Xu, and S. Jagannathan, "Localization of near-field radio controlled unintended emitting sources in the presence of multipath fading," *IEEE Trans. Instrum. Meas.*, vol. 63, no. 11, pp. 2696–2703, Nov. 2014.

[16] M. Scherhäufl, M. Pichler, D. Müller, A. Ziroff, and A. Stelzer, "Phase-of-arrival-based localization of passive UHF RFID tags," in *IEEE MTT-S Int. Microw. Symp. Dig. (IMS)*, Jun. 2013, pp. 1–3.

[17] M. Scherhäufl, M. Pichler, E. Schimbäck, D. J. Müller, A. Ziroff, and A. Stelzer, "Indoor localization of passive UHF RFID tags based on phase-of-arrival evaluation," *IEEE Trans. Microw. Theory Techn.*, vol. 61, no. 12, pp. 4724–4729, Dec. 2013.

[18] X. Li, Y. Zhang, and M. G. Amin, "Multifrequency-based range estimation of RFID tags," in *Proc. IEEE Int. Conf. RFID*, Apr. 2009, pp. 147–154.

[19] D. Arnitz, K. Witrisal, and U. Muehlmann, "Multifrequency continuous-wave radar approach to ranging in passive UHF RFID," *IEEE Trans. Microw. Theory Techn.*, vol. 57, no. 5, pp. 1398–1405, May 2009.

[20] A. Povalac and J. Sebesta, "Phase difference of arrival distance estimation for RFID tags in frequency domain," in *Proc. IEEE Int. Conf. RFID-Technol. Appl. (RFID-TA)*, Sep. 2011, pp. 188–193.

[21] Y. Ma and E. C. Kan, "Accurate indoor ranging by broadband harmonic generation in passive NLTL backscatter tags," *IEEE Trans. Microw. Theory Techn.*, vol. 62, no. 5, pp. 1249–1261, May 2014.

[22] R. Miesen, F. Kirsch, and M. Vossiek, "UHF RFID localization based on synthetic apertures," *IEEE Trans. Autom. Sci. Eng.*, vol. 10, no. 3, pp. 807–815, Jul. 2013.

[23] M. Scherhäufl, M. Pichler, and A. Stelzer, "Localization of passive UHF RFID tags based on inverse synthetic apertures," in *Proc. IEEE Int. Conf. RFID*, Apr. 2014, pp. 82–88.

[24] A. Parr, R. Miesen, and M. Vossiek, "Inverse SAR approach for localization of moving RFID tags," in *Proc. IEEE Int. Conf. RFID*, Apr./May 2013, pp. 104–109.

[25] A. Buffi, P. Nepa, and F. Lombardini, "A phase-based technique for localization of UHF-RFID tags moving on a conveyor belt: Performance analysis and test-case measurements," *IEEE Sensors J.*, vol. 15, no. 1, pp. 387–396, Jan. 2015.

[26] M. Scherhäufl, M. Pichler, and A. Stelzer, "UHF RFID localization based on phase evaluation of passive tag arrays," *IEEE Trans. Instrum. Meas.*, vol. 64, no. 4, pp. 913–922, Apr. 2015.

Martin Scherhäufl (S'12–GSM'14) was born in Linz, Austria, in 1981. He received the Dipl.-Ing. (FH) degree in sensors and microsystems from the University of Applied Sciences Upper Austria, Wels, Austria, in 2007. He is currently pursuing the Ph.D. degree with the Institute for Communications Engineering and RF-Systems, Johannes Kepler University Linz, Linz.

He was with the Department of Industry Automation, Siemens AG, Linz, from 2007 to 2009. Since 2009, he has been with the Department of Sensors and Communication, Linz Center of Mechatronics GmbH, Linz. His current research interests include system design, signal generation, digital signal processing, and RFID systems.

Markus Pichler (M'09) was born in Linz, Austria, in 1976. He received the Dipl.-Ing. degree in mechatronics and the Dr.Techn. degree from Johannes Kepler University Linz, Linz, in 2002 and 2007, respectively.

He was with the Institute for Communications and Information Engineering, University of Linz, Linz, where he joined the Linz Center of Mechatronics GmbH in 2002. He has authored or co-authored over 40 publications. His current research interests include systems design, signal generation, digital signal processing, and parameter estimation for radar and positioning systems.

Dr. Pichler was a recipient of the European Microwave Association Radar Prize in 2004.

Andreas Stelzer (M'00) was born in Haslach an der Mühl, Austria, in 1968. He received the Dipl.-Ing. degree in electrical engineering from the Technical University of Vienna, Vienna, Austria, in 1994, and the Dr.Techn. (Ph.D.) (Hons.) degree in mechatronics from Johannes Kepler University Linz, Linz, Austria, in 2000.

He became an Associate Professor with the Institute for Communications Engineering and RF Systems, Johannes Kepler University Linz, in 2003. Since 2007, he has been the Head of the Christian Doppler Research Laboratory for Integrated Radar Sensors. Since 2008, he has been a Key Researcher with the Austrian Center of Competence in Mechatronics, Linz, where he is responsible for numerous industrial projects. He has also been a Full Professor with Johannes Kepler University Linz since 2011, where he is currently the Head of the Department of RF-Systems. He has authored or co-authored over 320 journal and conference papers. His current research interests include microwave sensor systems for industrial and automotive applications, radar concepts, SiGe-based circuit design currently up to 320 GHz, microwave packaging in eWLB, RF, and microwave subsystems, surface acoustic wave sensor systems and applications, and digital signal processing for sensor signal evaluation.

Dr. Stelzer is a member of the Austrian Electrotechnical Association. He was a recipient of several awards, including the IEEE Microwave Theory and Techniques Society (IEEE MTT-S) Outstanding Young Engineer Award in 2008, and the IEEE Microwave Prize in 2011. Furthermore, he was also a recipient of the European Conference on Antennas and Propagation Best Measurement Paper Prize in 2012, the Asia Pacific Conference on Antennas and Propagation Best Paper Award in 2012, the German Microwave Conference Best Paper Award in 2011, the EEEfCOM Innovation Award, and the European Microwave Association Radar Prize of the European Radar Conference in 2003. He is a member of the IEEE MTT-S, the IEEE Instrumentation and Measurement Society, and the IEEE CAS Circuits and Systems Society. He has served as an Associate Editor of the IEEE MICROWAVE AND WIRELESS COMPONENTS LETTERS. He serves as the Co-Chair of the MTT-27 Wireless-Enabled Automotive and Vehicular Applications. He serves as the IEEE Distinguished Microwave Lecturer from 2014 to 2016.